

Reliability of Proposed Three-Dimensional Finite Element Method Prestressing Analysis

by Yasuaki Ishikawa, Tomoki Ito, and Satoshi Hayakawa

This paper examines the inaccuracy of the initial strain method that is generally adopted in three-dimensional (3-D) finite element prestressing analysis and discusses the merits of a newly developed method to calculate 3-D prestressing effects. The new method considers friction loss of the tendon force as well as pseudo-centripetal forces, allowing a wide range of functional forms for the prestressed concrete (PC) steel force distribution assumption. This study examined the basic concepts for adopting the functional form of the PC steel force distribution at the prestressing and seating stages, after which the observed and calculated values of pulled-out lengths of PC steel were compared to assure the credibility of the assumed functional form of the PC steel force distribution. A three-span continuous bridge model was used to compare results obtained by the conventional method and the new 3-D method. The equilibrium of a free body was used also to evaluate the accuracy of results by the new method. The importance of the new method being able to calculate a pulled-out PC steel length considering concrete deformation was stressed because this value may be adopted to confirm assumptions of the PC steel force distribution.

Keywords: free-body force balance; frictional force; pseudo-centripetal force; pulled-out prestressed concrete (PC) steel length.

INTRODUCTION

It might have been accepted in general that the stress calculation of structures due to prestressing of prestressed concrete (PC) steel with the three-dimensional (3-D) finite element method (FEM) has been already established¹⁻³ by applying the initial strain method. However, this notion comes up as incorrect when closely studying the adaptability of the initial strain method to prestressing analysis for arbitrary PC steel layouts and 3-D structures. A previous study³ clearly showed the inaccuracy of results with the initial strain method due to the introduction of PC steel rigidity to the overall stiffness matrix when it is applied directly without any modification, as done in the ABAQUS code. In contrast, the DIANA code considers the remedy that the PC steel rigidity be nullified when applying the initial strain method to calculate the prestressing load effect on concrete, while it fails when this remedy is applied to seating loss analysis.

Therefore, this study aimed at obtaining a more comprehensive prestressing analysis method for 3-D FEM calculation without using the initial strain method. The method developed is based on the principle that the prestressing load on concrete is given by the differential coefficient of the assumed PC steel force distribution on the local coordinates along the length of PC cable profiles. Then, the prestressing load on concrete through any PC cable profiles in the 3-D space is considered accurately, no matter the curvature

intensity and how large the number of PC cables. A computer code for general use that adopts the principle with 3-D FEM is now under development at the Japan Concrete Institute.

The developed 3-D FEM analysis treats the PC steel stress calculation separately from the concrete stress calculation and combines them only through the effect of forces acting mutually as action and reaction, because this problem is a non-conservative system in terms of mechanical energy. In other words, given the work of the prestressing jack force, $\int_{\Delta L_L} F_L \cdot dl + \int_{\Delta L_R} F_R \cdot dl$ is not equal to the summation of the mechanical energy stored in PC steel $A_s \int_x \left(\int_{\epsilon_s} \sigma_s d\epsilon_s \right) dx$ and in concrete $\int_{V_c} \left(\int_{\epsilon_c} \sigma_c^T d\epsilon_c \right) dV_c$, where F_L , F_R , ΔL_L , ΔL_R , A_s , x , σ_s , and ϵ_s stand for jack forces at the left and right sides, PC steel elongations at the left and right jack points, the PC steel area, the PC steel length, the PC steel stress, and the PC steel strain, respectively. In addition, σ_c , ϵ_c , and V_c denote the concrete stress tensor, concrete strain tensor, and volumetric domain of concrete, respectively. The integral should cover the area between jack point and fixed unmovable point in a PC steel, which is defined in detail in the section "PC steel force expression with polylinear approximation of the cable profile." More correctly, the work generated by the jack force exerted on PC steel is not equal to the mechanical energy stored in PC steel; it is, however, equal to the summation of the mechanical energy stored and energy consumed by friction between PC steel and concrete, including thermal energy. In other words,

$$\int_{\Delta L_L} F_L \cdot dl + \int_{\Delta L_R} F_R \cdot dl = A_s \int_x \left(\int_{\epsilon_s} \sigma_s d\epsilon_s \right) dx + \int_{V_c} \left(\int_{\epsilon_c} \sigma_c^T d\epsilon_c \right) dV_c + Q \quad (1)$$

where Q stands for the energy consumed by friction between PC steel and concrete, including the thermal energy generated during prestressing. However, as for the number of Q values for prestressing, it is hard to find an appropriate friction law: for instance, Coulomb's law of friction seems completely inapplicable to concrete prestressing. Therefore, this problem was ignored in this study. Instead, it was assumed, as in the past, that PC steel stress reduction due to friction is linearly dependent on the force working at each

ACI Structural Journal, V. 122, No. 2, March 2025.

MS No. S-2023-218.R2, doi: 10.14359/51744393, received June 25, 2024, and reviewed under Institute publication policies. Copyright © 2025, American Concrete Institute. All rights reserved, including the making of copies unless permission is obtained from the copyright proprietors. Pertinent discussion including author's closure, if any, will be published ten months from this journal's date if the discussion is received within four months of the paper's print publication.

point of PC steel. In other words, adoption of the differential equation $\partial T/\partial s = -f(s)T$ is judged to be an appropriate expression in light of past experience with prestressing. Once this differential equation is adopted, the PC steel stress distribution is decided uniquely in any configuration of cable profiles, and the prestress loading is given by differentiating the PC steel force distribution. These formulations are shown in the following sections. The PC steel stress distribution that is affected by friction is vital not only during prestressing but also at the seating stage. The authors consider that the assumed stress distribution of PC steel affected by friction may be verifiable through the comparison of the observed and the calculated result of the pulled-out lengths of PC steels with an assumed PC steel force distribution because the theoretical calculation of pulled-out lengths of PC steel has been enabled by this study, as described in the next section.

In this paper, the proposed theoretical development is elaborated first and then the accuracy of the results of the developed 3-D FEM calculation is discussed in comparison with results of the conventional method assuming the same PC steel force distribution. Furthermore, it is shown that the adoption of a 3-D strain calculation enabled the derivation of the PC steel length that is pulled out from an anchorage plate during prestressing, as well as that of the opposite pulled-out length that occurs during the seating stage.

RESEARCH SIGNIFICANCE

This study provides an improved fundamental theory of PC steel prestressing analysis on a 3-D FEM platform, which may replace the initial strain method or initial stress method that are currently used. Further, some proofing examples are shown. It is explained that the non-conservative character of mechanical energy due to friction loss leads to an appropriate assumed PC steel force distribution function. It is stressed that the seating analysis is fully developed, and its stress relief calculation agrees well with observed values from an existing bridge.

CALCULATION OF PC STEEL FORCES

Derivation of frictional force and pseudo-centripetal force

As is mentioned in the introduction, adoption of the differential equation $\partial T/\partial s = -f(s)T$ as the governing rule for the PC steel force distribution is essential for non-conservative systems because the energy consumed by friction is not known, and some rules should be assumed for the PC steel strain distribution in the first step. Although the differential equation form is adopted, the assumption of a formula for the strain distribution along the PC steel profile is not necessary; it is given as a solution of the assumed differential equation.

In current practice, $f(s) = \mu\partial\theta/\partial s + \lambda$ is adopted and its solution, $T = T_0 \cdot e^{-\mu\theta - \lambda s}$ is generally adopted. Furthermore, the current practice in 3-D FEM is to adopt the initial strain method to obtain the prestressing load on concrete using the PC steel strain distribution $T = T_0 \cdot e^{-\mu\theta - \lambda s}$, as found in ABAQUS or DIANA, similar to the case of thermal load. However, it is noted that the initial strain method gives inaccurate results³ when the relative rigidity of PC steel becomes

large compared with that of concrete. Therefore, DIANA uses the remedy that the PC steel rigidity is null during the prestressing stress calculation for concrete. However, those main software packages have shown deficiencies when the seating stage analysis is compared with actual measurements of PC steel strains in an existing six-span highway bridge.^{4,5}

This study proposes a new prestressing analysis method as follows. For the PC steel force, a general form for the governing differential equation is assumed, such as

$$\frac{\partial T}{\partial s} = -f(s)T \quad (2)$$

and its solution is given as

$$T = T_0 \cdot e^{-\int f(s)ds} \quad (3)$$

where T and T_0 denote the PC steel force at local coordinate location s and the PC steel force at the end where a prestressing jack is working. The only limit of the method is the integrability of $f(s)$.

Because the PC steel force is a vector, the previous expression can be written as

$$\mathbf{T} = T_0 \cdot e^{-\int f(s)ds} \cdot \mathbf{n} = T(\theta, s) \cdot \mathbf{n} \quad (4)$$

where \mathbf{n} is a unit tangential vector that can be defined at every point of the PC steel profile.

The form $f(s)$ allows for a wide range of functions because the computer code under development can treat the integration numerically. Force vectors \mathbf{f} working on the concrete are the variation of the PC steel force and given by the differential coefficient of the local length coordinate measured from an end along a cable profile

$$\mathbf{f} = \frac{\partial \mathbf{T}(\theta, s)}{\partial s} = \frac{\partial (T(\theta, s) \cdot \mathbf{n})}{\partial s} = \frac{\partial T(\theta, s)}{\partial s} \cdot \mathbf{n} + T(\theta, s) \cdot \frac{\partial \mathbf{n}}{\partial s} = \mathbf{S} + \mathbf{Z} \quad (5)$$

where

$$\mathbf{S} = \frac{\partial T(\theta, s)}{\partial s} \cdot \mathbf{n} \quad (6)$$

and

$$\mathbf{Z} = T(\theta, s) \cdot \frac{\partial \mathbf{n}}{\partial s} \quad (7)$$

The first term on the right-hand side of Eq. (5) is frictional force, and the second term is pseudo-centripetal force. As for the unmovable fixing point of a PC steel, PC steel cables are tensioned by exerting jacking forces at both ends. During the process, the PC steels are pulled out of the anchorage plate at the concrete surface at both ends. However, there exists one unique point in a PC steel, where slip relative to the concrete does not occur and the steel and concrete do not move relative to each other during the prestressing process. In other words, there is a point where relative displacement between concrete point and prestressing PC steel material point does

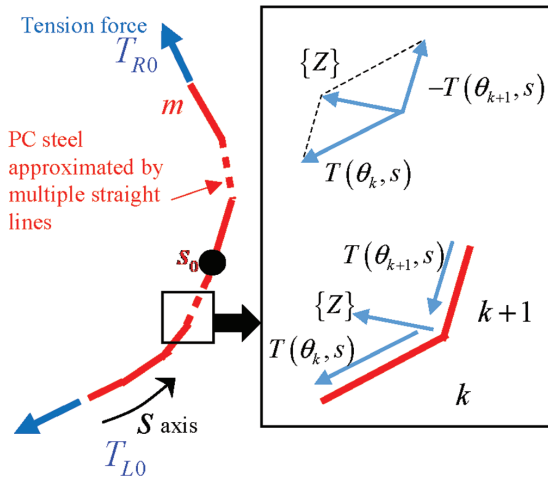


Fig. 1—Curved PC steel cable approximated by multiple straight lines.

not occur throughout the tensioning process. This point is called the unmovable fixing point of a PC steel.

PC steel force expression with polylinear approximation of the cable profile

For numerical treatment, a curved PC steel in 3-D space is approximated by multiple straight lines and modeled as series of line groups composed of m line segments, as shown in Fig. 1, the size of which depends on the required accuracy of its solution. The length of m line segments is generally not equally divided, and it is necessary to divide it depending on the PC steel curvature radius. In a domain where the curvature radius is small, it is necessary to increase the number of divisions and use short line segments. Note that both ends of each line segment need not be on the surface of solid elements of concrete. Let coordinate s along the line segment be taken from the left end of a PC steel and let θ_k be the sum of the angles formed by line segments $k+1$ from the left end, where angles are measured clockwise. Then, the unmovable fixing point s_0 satisfies the following equation by its definition

$$T_{L0} \cdot \exp\{-f(\theta_k, s_0)\} = T_{R0} \cdot \exp\{-f(\theta_{m-k}, (s_{max} - s_0))\} \quad (8)$$

So far, the written the PC steel force has been written as $T = T_0 \cdot f(\theta_k, s)$ with an initial assumption of the frictional characteristics. Applying the bisection method to Eq. (8) and performing iterative calculations obtains the unmovable fixing point s_0 numerically. The tension force $T(\theta_k, s)$ generated in the PC steel can now be expressed by the following equations by using the unmovable fixing point as the domain boundary

$$T(\theta_k, s) = \begin{cases} T_{L0} \cdot \exp\{-f(\theta_k, s)\} & s \leq s_0 \\ T_{R0} \cdot \exp\{-f(\theta_{m-k}, (s_{max} - s))\} & s > s_0 \end{cases} \quad (9)$$

where s_{max} is the total line group length or the total length of the single PC steel of concern.

It is clear that either the left or right end of the PC steel will be the unmovable fixing point if the PC steel is pulled from one side alone. The friction forces $\{S\}$ along the PC steel configuration direction, Eq. (6), can be rewritten with polylinear approximation as

$$\{S\} = \frac{\partial T(\theta_k, s)}{\partial s} \{n_k\} \quad (10)$$

where $\{n_k\}$ denotes the unit vector for the direction of line segment k .

When an angle change occurs between line segment k and line segment $k+1$, as shown in Fig. 1, pseudo-centripetal force $\{Z\}$ is generated at the point where these line segments are connected. From Eq. (7), $\{Z\}$ is written as

$$\{Z\} = T(\theta_k, s) \{n_k\} - T(\theta_{k+1}, s) \{n_{k+1}\} \quad (11)$$

Conversion of PC steel forces into equivalent nodal force of concrete

Based on Eq. (9), equivalent nodal forces are derived for the FEM calculation from the frictional force of PC steels and from pseudo-centripetal forces due to the angle change of line segments. Reaction forces $\{R\}$ exerted on concrete elements at the left and the right PC steel ends by the tension forces are opposite-sign forces of the tension forces T_{L0} and T_{R0} at the ends, and its nodal forces can be obtained by applying the virtual work principle. The increment of equivalent nodal force $\{Q\}$ can be finally given as

$$\{Q\} = [N]^T [\{R\} + \{Z\}] + \int_s [N]^T \frac{\partial T(\theta_k, s)}{\partial s} \{n_k\} ds \quad (12)$$

where $[N]$ is the shape function of a solid element of concrete.

Although Eq. (12) includes a path integral with respect to s , it should be noted that, in the segment where the unmovable fixing point exists, the path integral must be divided into cases with the fixing point as the boundary. The path integral in Eq. (12) can be easily calculated by a previously reported numerical integration method.⁶

Calculation of pulled-out PC steel length from anchor plate considering concrete deformation

Seating analysis of PC steels is a problem to obtain the stress distribution under the condition of given pulled-out lengths of PC steels with a negative sign. ABAQUS does not have answers for the problem, while DIANA recommends in its manual to only assume a kind of mirror inversion of the PC steel force relief at certain lengths from the anchor plates but provides no assurance that the given condition of the pulled-out length of PC steels is accurately satisfied. The difference between the DIANA solution compare to the measured values will be shown in later in this section.

To begin the formulation, first treat the pulled-out length calculation at prestressing. Lengths of PC steel pulled out from anchor plates at the left and the right ends are expressed by the following equations, where the lengths at the left and the right ends are denoted as $\Delta \ell_L$ and $\Delta \ell_R$, respectively

$$\Delta\lambda_L = \Delta\ell_{L,cab} - \Delta\ell_{L,con}, \Delta\ell_R = \Delta\ell_{R,cab} - \Delta\ell_{R,con} \quad (13)$$

in which subscripts *cab* and *con* denote components of the pulled-out length attributed to the PC steel extension and concrete deformation, respectively. The left and the right pulled-out PC steel length components attributed to PC steel can be expressed by the following equations, respectively, by the path integral of the strain generated in the PC steel along the PC steel length starting from the unmovable fixing point to the left end or to the right end

$$\Delta\ell_{L,cab} = \int_0^{s_0} \frac{T(\theta_k, s)}{EA} ds, \Delta\ell_{R,cab} = \int_{s_0}^{s_{max}} \frac{T(\theta_k, s)}{EA} ds \quad (14)$$

where *EA* is the axial stiffness of PC steel.

In addition, the left and right pulled-out PC steel length components due to concrete contraction are expressed by Eq. (15a) and (15b), respectively, by the path integral of concrete strain components along the PC steel from the unmovable fixing point to the left or right end.

$$\Delta\ell_{L,con} = \int_0^{s_0} \varepsilon_c ds, \Delta\ell_{R,con} = \int_{s_0}^{s_{max}} \varepsilon_c ds \quad (15)$$

where ε_c is the normal strain component of concrete in the direction along the PC steel and is expressed by Eq. (16) using concrete strain tensor ε_{ij} and the component n_i of the unit vector $\{n_k\}$, which is the PC steel profile directional normal to a PC steel point.

$$\varepsilon_{\chi} = \varepsilon_{ij} n_j n_i \quad (16)$$

The path integral in Eq. (14) can also be performed by a previously reported method.⁶

The formulation at the seating stage is next. The previous derivation is used in both the prestressing stage and seating stage. However, the unknown parameters are different at the seating stage. At the prestressing stage, the unknown parameters are the pulled-out lengths, Δl_R and Δl_L , while they are T_{R0} and T_{L0} at the seating stage, or the prestressing forces at both ends. For the seating problem, it is obvious that iteration is necessary when a calculated pulled-out length is different from a given length, in such a way that the strain relief assumption must be modified according to the differences of the calculated pulled-out and given lengths. The proposed method performs the iteration until the limiting convergence is attained. It is stressed that it is important to recognize at least three factors in the seating stage—namely, the PC steel force distribution affected by different friction intensities, movement of the fixing point from the prestressing stage at which the PC steel forces from both sides become balanced, and concrete contraction. Each of these will be discussed rather briefly in the following. They are treated in more detail elsewhere.⁷

PC steel force distribution affected by different friction intensity at seating stage

The basic assumption of the PC steel force distribution is that the governing differential equation of the PC steel force expressed as Eq. (2) does not change even at the seating stage.

In other words, superposition of the solution exists even at the seating stage. However, the concrete form of $f(s)$ is still under examination, as mentioned before, and this study adopted the one that gives the least square error because the authors have tools to calculate the pulled-out lengths of PC steels once the PC steel force distribution assumption is adopted.

So far, the least square of error dispersion looks reasonably small in the assumed PC steel stress distribution as

$$f(s) = f^*(s/s_0^*) = \mu \left(\frac{1}{s_0^*} \right) \frac{\partial \theta}{\partial s} + \lambda \left(\frac{1}{s_0^*} \right) \quad (17)$$

Then, $T(s)$ is expressed as

$$T(s) = T_0 \cdot e^{-\mu \theta \left(\frac{s}{s_0^*} \right) - \lambda \left(\frac{s}{s_0^*} \right)} \quad (18)$$

This is the normalized form of the formula currently adopted at the prestressing stage, and if one takes $s_0^* = 1$ m, it reduces to

$$f(s) = f^*(s/1 \text{ m}) = \mu \frac{\partial \theta}{\partial s} + \lambda \quad (19)$$

The normalization by s_0^* of the original length s for the PC steels is understood to express the contact point density. This study used the value $s_0^* = 1$ m at the prestressing stage and $s_0^* = 3.3$ cm at the seating stage, according to the increase of contact density. Again, the reliability of the assumed PC steel force distribution will be confirmed by comparing the specified and calculated pulled-out lengths of PC steels.

Movement of fixing point from prestressing stage

At the seating stage, in Eq. (9), T_{L0} and T_{R0} will take different values from those of the prestressing stage. Therefore, the fixing point location s_0 changes.

Concrete contraction

Concrete contraction or stress relief at the seating stage $\varepsilon_c = \varepsilon_{ij} n_j n_i$ is recalculated, and Eq. (15) is applied with a renewed integration domain because the fixing point has changed. It should be noted herein that if a PC steel is in the air, integration of Eq. (15) may be replaced with the displacement between the points where a PC steel leaves the concrete and enters air at a point A, where $s = s_{R, \text{in air}}$, and reaches the other side of concrete at a point B, where $s = s_{L, \text{in air}}$ in such a way that

$$\int_{s_{L, \text{in air}}}^{s_0} \varepsilon_c ds + \int_{s_0}^{s_{R, \text{in air}}} \varepsilon_c ds = \int_{s_{L, \text{in air}}}^{s_{R, \text{in air}}} \varepsilon_c ds = \Delta_{\text{air}} \quad (20)$$

$$\Delta_{\text{air}} = (l - l_0) \quad (21)$$

where

$$l = \sqrt{(x_B + u_B - x_A - u_A)^2 + (y_B + v_B - y_A - v_A)^2 + (z_B + w_B - z_A - w_A)^2} \quad (22)$$

and

$$l_0 = \sqrt{(x_B - x_A)^2 + (y_B - y_A)^2 + (z_B - z_A)^2} \quad (23)$$

Herein, (x_A, y_A, z_A) are coordinates for A; (x_B, y_B, z_B) are for B; and $\mathbf{u}_A = (u_A, v_A, w_A)$ and $\mathbf{u}_B = (u_B, v_B, w_B)$ are the displacements of points A and B, respectively. Alternatively, air elements may be used to calculate the integration.

COMPARISON OF 2-D FRAME ANALYSIS AND 3-D FEM MODELING OF PRESTRESSING EFFECTS FOR THREE-SPAN CONTINUOUS BRIDGE

The purpose of this comparison is to show agreement of the calculation results of the two-dimensional (2-D) frame analysis currently used worldwide with those of the proposed 3-D FEM analysis, when both analyses use the same PC steel force distribution assumption. It should be noted that 2-D frame analysis generally assumes the PC steel stress distribution as⁸

$$T = T_0 \cdot e^{-(\mu\theta + \lambda s)} \quad (24)$$

Therefore, the proposed method also assumed the same PC steel force distribution, although this method and its computer code can treat any kind of PC steel force distribution, as mentioned in the previous section. Depending on the purpose of the analysis, various tension formulas, including those given in the literature,⁹ can be adapted.

The subsequent calculations were carried out with the 3-D FEM code LECOM to implement the proposed analytical method. LECOM was developed by the LECOM Research Association¹⁰ in Japan and knowhow obtained with LECOM has been under continuous implementation for the JCMAC3 software of the Japan Concrete Institute.

Three-span continuous bridge model

The adopted bridge configuration is shown in Fig. 2, where the sectional dimensions of box girders as well as the solid sections of piers are shown, and six prestressing PC steels are deployed with 2900 kN of prestressing force per PC steel cable, and all PC steels are arranged through the bridge length from the one end to the other. Mesh discretization for the 3-D FEM analysis was performed with almost cubic solid elements measuring 40 cm throughout the whole structure, and the number of degrees of freedom amounted to approximately 165,000.

Calculation of deformation and sectional forces

Applied forces are the dead load and the prestressing force, and these are applied separately. Sectional forces and moments are shown in Fig. 3, where the red curves are the prestressing force, the blue curves are the dead load of the bridge's own weight, and each numeric number with U and N denotes the results by the 2-D frame analysis and the proposed 3-D FEM, respectively. Figure 4 shows the calculation results of deflection, where the upper figure is the deflection by the dead load and the lower figure shows deflection by the prestressing force. It is important to note that the response of the bridge to the dead load is nothing less than the comparison of the general 2-D frame analysis and 3-D FEM analysis; while for the response to prestressing force, the treatment of the frictional effect is different between the two, the comparison has its own meaning, and they produce

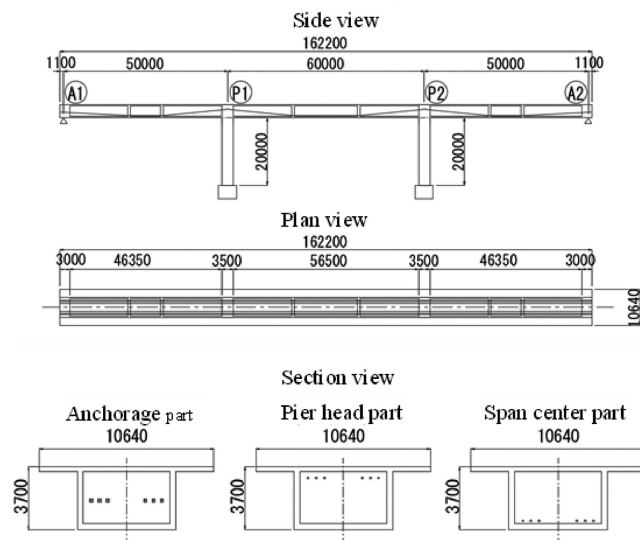


Fig. 2—Configuration of three-span continuous bridge.

almost the same results except for the deflection that gives a 13 to 38% increase for the 3-D FEM with respect to the results of the 2-D frame analysis, as shown in Table 1. This difference is caused by shear deflection, which is neglected in the 2-D frame analysis but not the 3-D FEM calculation. This is shown by calculating the shear deformation by simply applying the Timoshenko beam theory. In other words, the shear strain of the section is adopted as

$$\gamma = \frac{\kappa S}{GA} \quad (25)$$

where κ is a factor that depends on the box configuration; S and A are the shear forces acting on a section and sectional area, respectively; and G is the shear rigidity. The differences of the results of the two calculation methods almost agree with the calculated shear deformation in every case when $\kappa = 4$ is assumed,¹¹ as shown in Table 1. For the different values of κ , agreement may become less than that in Table 1, but the κ value is limited to roughly 2 to 5, and it may be obvious that shear deformation is the predominant factor of the deformation difference between the two calculation methods.

Another examination to assure reliability of the proposed method of calculation is found in the value of the prestressing force of the PC steel at the central span center, which must agree with the value of the given jack prestressing force minus frictional forces along the PC steel length from one end to the center point of the bridge—that is, 14,968 kN, which is the value calculated by $T = T_0 \exp(-\mu\theta - \lambda s)$ with a small amount of error due to the approximated segment assembly of the curved PC steel profile. The corresponding value by the 2-D frame analysis is 14,716 kN and the difference from the 3-D FEM is 252 kN, which is reasonably small, though it may be safely said that the difference is mostly attributable to the error of the 2-D frame analysis.

EXAMINATION USING EXISTING SIX-SPAN BRIDGE DATA

The data used was obtained during construction of a 462 m long six-span viaduct to evaluate the reliability of the

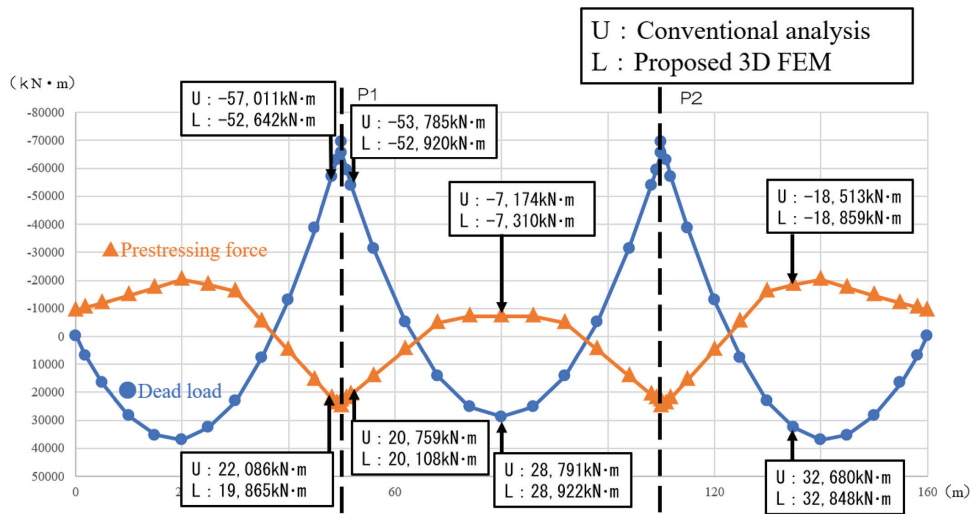


Fig. 3—Comparison of obtained bending moments from conventional analysis and from proposed 3-D FEM.

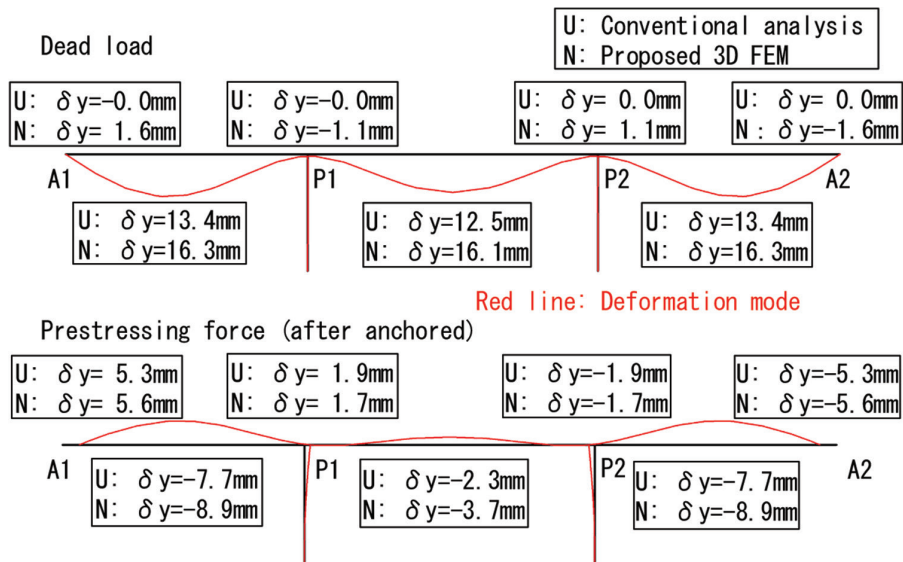


Fig. 4—Comparison of vertical deflections calculated by conventional analysis and by proposed 3-D FEM.

proposed method. Note that a study of the existing bridge was already reported in detail in Nishio et al.¹² and only the portions related to force balance, strain measurements, and pulled-out lengths are discussed in this paper.

Figure 5 shows shape of the existing bridge, namely the longitudinal and plan views. With a total length of 462 m, the curved line is approximately 12 m away from the straight line connecting A1 and A2 at the point of greatest curvature. There exists an elevation difference of approximately 5 m between points A1 and A2 due to a longitudinal gradient. Table 2 shows the dimensions of the bridge.

Prestressing PC steel with built-in optical fibers in the external cables^{4,5} was specially arranged between piers P2 and P4 and between piers P1 and P2, and the tension force in the PC steel at prestressing was measured. Figure 6 shows the model diagram of the bridge and a part of the discretization. Table 3 shows the parameters used for the analysis. Because the bridge draws a gentle s-curve on the plane and has a gentle upward slope from points A1 to A2, the arrangement of the prestressing PC steel is not symmetric.

Table 1—Comparison of vertical deflections by proposed 3-D FEM, conventional analysis, and Timoshenko shear deflection, mm

Load	Position	Proposed method	Conventional method	Difference	Calculated shear deflection
Dead load	Center span	16.1	12.5	3.6	3.7
	Side span	16.3	13.4	2.9	2.8
Prestressing force by external cables	Center span	-3.7	-2.3	-1.4	-1.2
	Side span	-8.9	-7.7	-1.2	-1.1

The entire 462 m long six-span bridge was faithfully discretized, as shown in Fig. 6. Therefore, the model provided a large degree-of-freedom analysis, with 257,566 elements, 367,271 nodes, and 1,101,813 degrees of freedom.

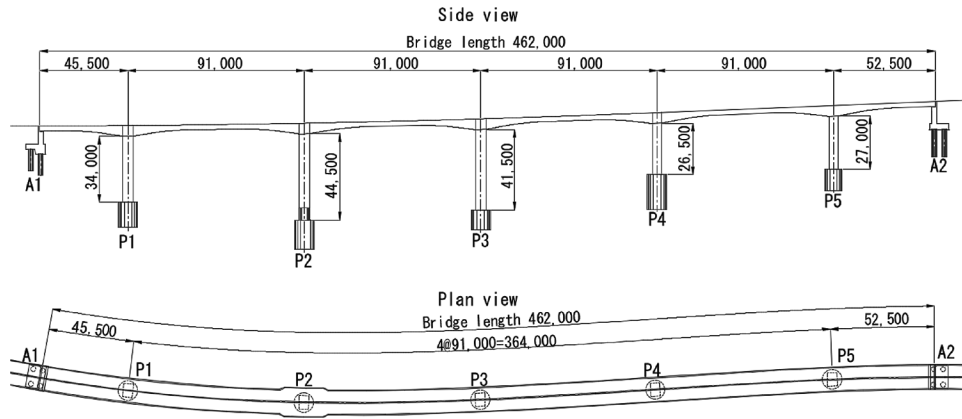


Fig. 5—General view of existing continuous viaduct.^{9,10}

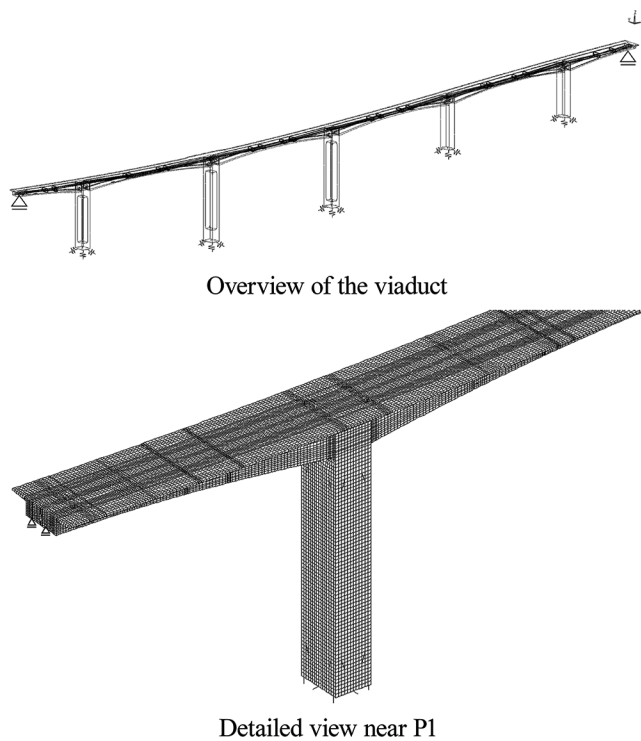


Fig. 6—3-D discretization model for proposed method.

Sectional forces calculated using free-body force balance

In 3-D FEM analysis, stress is calculated based on strain, which comes from displacement, and the cross-sectional force is obtained by integrating this stress. In other words, there are two steps in the middle of the procedure. In contrast, a method of calculating cross-sectional forces using free-body equilibrium gives cross-sectional forces and moments from the balance of the three axial forces and the three moments around three axes due to existing external and reaction forces only at the pier bases. Then, the middle of the procedure has only one step, which is expected to increase the accuracy of the obtained values. Therefore, the sectional forces and moments derived from stress integration of a section of the 3-D FEM model were compared with the ones derived from the free-body equilibrium calculation of the 3-D FEM. Two prestressing cases were used in the aforementioned bridge construction, where the PC

Table 2—Overview of existing continuous viaduct

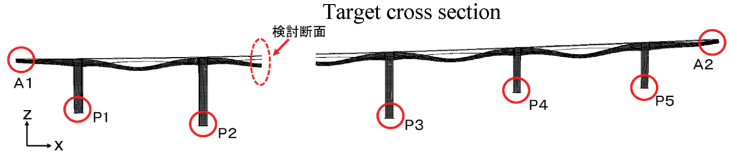
Bridge type	Prestressed concrete box girder bridge
Structural form	Six-span continuous rigid-frame viaduct
Bridge length	462.000 m (road center)
Span length	44.500 + 4 × 91.000 + 51.500 m (structural center)
Width	12.800 to 15.300 m
Effective width	5.565 + 5.565 to 6.815 + 6.815 m
Alignment of bridge	Longitudinal gradient: +3.007% (L = 470.000 m)
	Cross slope: 1.886% – 6.000%
	Plane figure: A = 400 to 450 m (clothoid), R = 900 m (arc)

Table 3—Parameters used for analysis

Young's modulus	Concrete (superstructure)	31,000 N/mm ²
	Concrete (substructure)	28,000 N/mm ²
	Prestressing steel (from mill sheet)	194,150 N/mm ²
Coefficient of friction	Per length	0.0/m
	Per angle	0.3/rad
Analysis model	Number of nodes	367,271
	Number of elements	257,566

steel strains were actually measured. One is the PC steel prestressing between piers P2 and P4 in Fig. 5. The other is the PC steel prestressing between piers P1 and P2 in Fig. 5. In the former case, a free body was composed to cut through the center cross section between P2 and P3. This cross section was used as the examination cross section, which is near cross section 66 in Fig. 7. When the portion of the bridge from A1 to the cross section, which includes A1, P1, and P2, was considered as a free body, the cross-sectional force at that section was calculated from the balance of the six components of the forces and moments acting on this free body; in other words, the sum of three orthogonal axial force components and three orthogonal moments around any point in 3-D space must be zero in total. Table 4 shows a comparison between this derived cross-sectional force and the cross-sectional force obtained by the integration of stresses obtained by the proposed method. The two are in

Table 4—Cross-sectional forces obtained from free-body force balance and from proposed method



Force	Nx, kN	Ny, kN	Nz, kN	Mx, kN·m	My, kN·m	Mz, kN·m
Cross-sectional force obtained from balance of forces and moments that act on free body	-27,904	-406	-545	-212	10,773	-1617
Cross-sectional force obtained from proposed method	-28,259	-399	-559	-222	10,912	-1625

Table 5—Cross-sectional forces obtained from free-body force and moment balance and from proposed method

Force	Nx, kN	Ny, kN	Nz, kN	Mx, kN·m	My, kN·m	Mz, kN·m
Cross-sectional force obtained from balance of forces and moments acting on free body	-7375	577	-26	261	3501	809
Sectional force obtained from proposed method	-7379	577	-29	260	3474	808

good agreement, confirming the reliability of the proposed method. In the latter case, a free body was formed to cut through the cross section between sections 32 and 33 in Fig. 7. The free body was the portion of the bridge from A1 to the cross section, with includes A1 and P1. Similar to the six components of sectional forces due to the external cables shown in Fig. 7, the three-directional axial forces and the moments around the three-directional axes were calculated and shown in Table 5. They are all in good agreement. This indicates that the proposed method accurately calculates the sectional forces acting on the curved bridge. This should be true no matter what PC steel force distribution assumption is adopted.

Comparison of strain distribution of PC steel during tensioning between observation and calculation results

Figure 8 shows the arrangement of the PC steel at the pier P1 head, where the first block is cantilevered. PC steels U100-1L and U100-1R are located in the left and the right webs, and PC steels U100-2L and U100-2R are located in the upper slab. Figure 8 also shows the arrangement of PC steels cantilevering the fourth block from the pier P1 head, and those PC steels, U104-L and U104-R, are located in the left and right webs. The PC steel layout in the bridge is shown in Fig. 8 with red lines. Mesh models are shown in Fig. 9 with the final tension forces measured during the actual construction, which were used in the analysis.

Strain measurement results with their distribution in the PC steel, as well as the pulled-out PC steel length at the jack position, are compared with the calculated results adopting the PC steel force variation of $T = T_0 \cdot e^{-\mu(1/s_0)\theta - \lambda(1/s_0)s}$ with $s_0^* = 1$ m.

Figure 10 shows the comparison of the measured and calculated tension forces at the pier P1 cap as an example. The measured strain is in the web PC steel U100-1L. Although fluctuation exists in the measured values, the strain

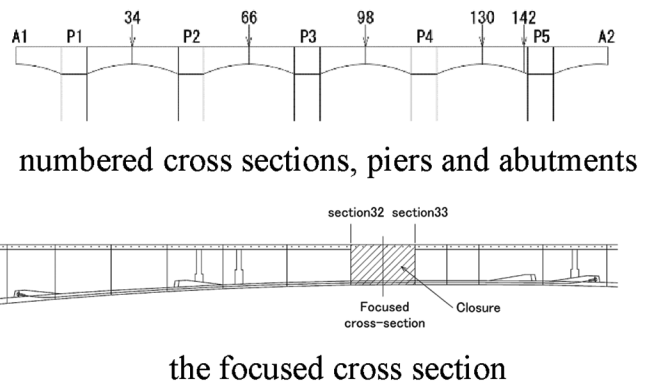


Fig. 7—Locations and identification numbers of cross sections, piers, and abutments and cross section focused on in this study.

distribution decreases slightly toward the center of the PC steel due to friction loss, which looks surprisingly small. The analysis results also show the effect of friction loss. Design values for friction by the Japan Road Association⁸ are 0.3 for μ and 0.004 for λ , values that we concluded were too large for this case. In the calculation, μ values were varied from 0.01 to 0.3 while keeping $\lambda/\mu = 0.0133$. Comparison of the measured and analytical values indicates that the actual friction coefficient is small and on the order of 10^{-2} .

Tables 6 and 7 show measured values of the pulled-out PC steel length at jack positions of the PC steels and analytical values by the proposed method. The measured values and the analytical values of the PC steels of the web and the slab at the pier P1 head, as well as at the stage of the overhanging fourth block, become closer in agreement when the friction coefficient $\mu = 0.01$ or less is assumed for all the PC steels discussed herein.

Seating analysis of PC steels

The pulled-out lengths during prestressing and seating were measured for the external cable between spans P2 and

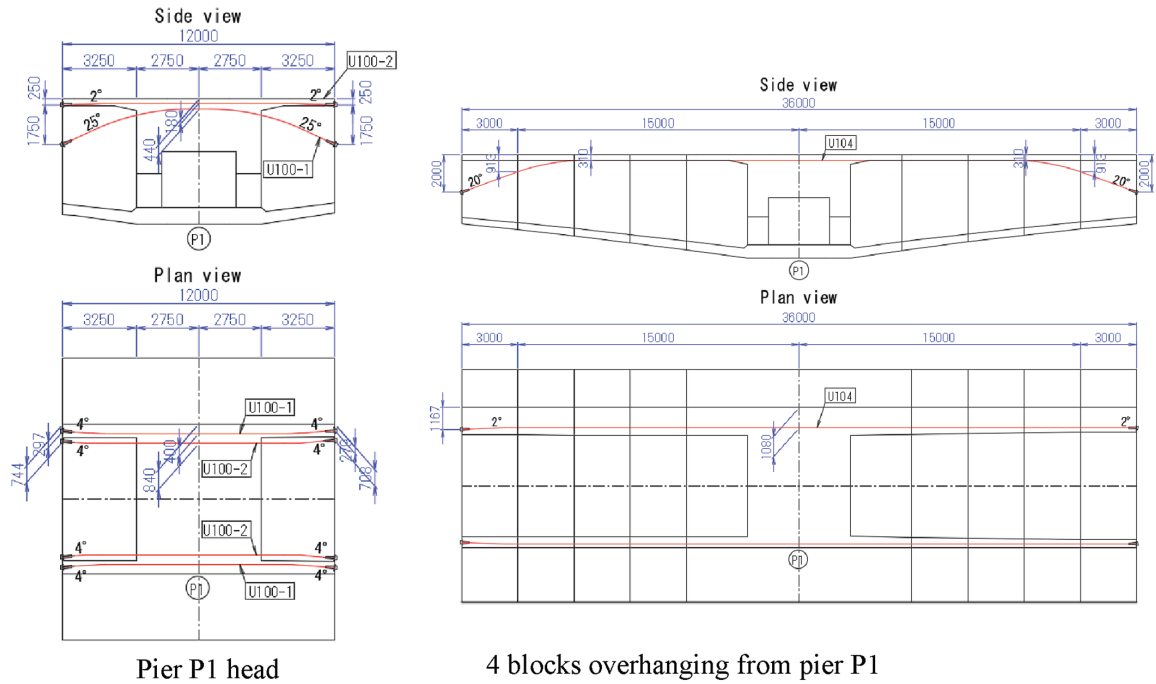


Fig. 8—Locations of PC steel cables.

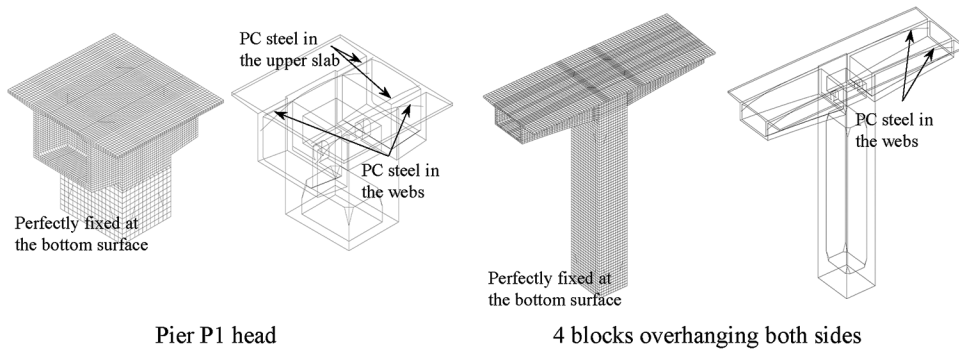


Fig. 9—Mesh discretization and locations of PC steel cables.

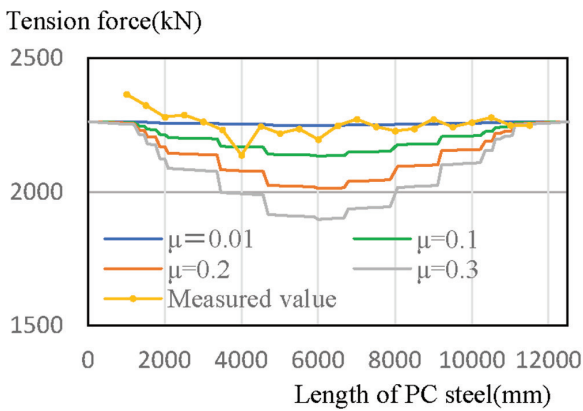


Fig. 10—Frictional coefficient and tension force distribution of PC steel in web at pier P1 head.

P4 and for internal cables between spans P1 and P2. PC steel was pulled out from anchor plate during prestressing, and its observed pulled-out length was compared with the calculated lengths. To calculate the pulled-out length of steel, concrete contraction must be calculated, which is not accurately evaluated in current practice. This study showed

how to calculate it accurately for both cases where PC steels are embedded in concrete, the so-called internal cables, and for PC steel suspended in the air, the external cable in the previous section. It is also emphasized that the pulled-out length calculation of PC steel in the air is generally also applicable to cable-stayed bridge or extradosed cable bridge calculations. Figure 11 shows the PC steel profiles between spans P2 and P4 and for the internal cables of span P1-P2. Table 8 shows the analytical conditions. The measured pulled-out lengths before seating are compared with calculated results for the external cable prestressing between span P2-P4 as an example.

Figure 12 shows the comparison between the measured tension force in the prestressing PC steel and the analytical pulled-out length for various friction coefficients. It shows perfect agreement of both values when we adopt $\mu = 0.3$, $\lambda = 0.003$, and $s_0^* = 1$ m, producing a steel force variation of

$$T = T_0 \cdot e^{-\mu \left(\frac{l}{s_0^*}\right) \theta - \lambda \left(\frac{l}{s_0^*}\right) s} \quad (26)$$

In Fig. 13(a), the measured tension force distribution after seating is shown, which indicates that the strain relief zone

Table 6—Measured values of pulled-out steel length and analytical values by proposed method in web and slab at pier P1 head, mm

Cable location	Measured value			Analytical value $\mu = 0.01$ $\lambda = 0.000133$			Analytical value $\mu = 0.1$ $\lambda = 0.00133$			Analytical value $\mu = 0.2$ $\lambda = 0.00266$			Analytical value $\mu = 0.3$ $\lambda = 0.004$		
	Side A1	Side A2	Total	Side A1	Side A2	Total	Side A1	Side A2	Total	Side A1	Side A2	Total	Side A1	Side A2	Total
Left side web (U100-1L)	46.5	77.5	94.0	42.9	48.4	91.3	41.8	47.2	89.0	40.7	45.9	86.6	39.5	44.6	84.1
Right side web (U100-1R)	46.6	41.6	88.2	47.6	40.6	88.2	46.4	39.7	86.1	45.1	38.7	83.8	43.9	37.7	81.6
Left side slab (U100-2L)	41.6	44.6	86.2	34.6	50.0	84.6	34.3	49.5	83.8	33.9	49.0	82.9	33.5	48.5	82.0
Right side slab (U100-2R)	40.6	44.6	85.2	34.2	50.4	84.6	33.9	49.9	83.8	33.5	49.4	82.9	33.2	48.9	82.1

Table 7—Measured values of pulled-out steel length and analytical values by proposed method at fourth cantilevered block at pier P1 head

Cable location	Measured value			Analytical value $\mu = 0.01$ $\lambda = 0.000133$			Analytical value $\mu = 0.1$ $\lambda = 0.00133$			Analytical value $\mu = 0.2$ $\lambda = 0.00266$			Analytical value $\mu = 0.3$ $\lambda = 0.004$		
	Side A1	Side A2	Total	Side A1	Side A2	Total	Side A1	Side A2	Total	Side A1	Side A2	Total	Side A1	Side A2	Total
Left side (U104-L)	124	122	245	132	129	261	127	124	251	122	119	241	117	115	232
Right side (U104-R)	137	107	243	133	132	265	129	127	256	124	122	246	119	118	237

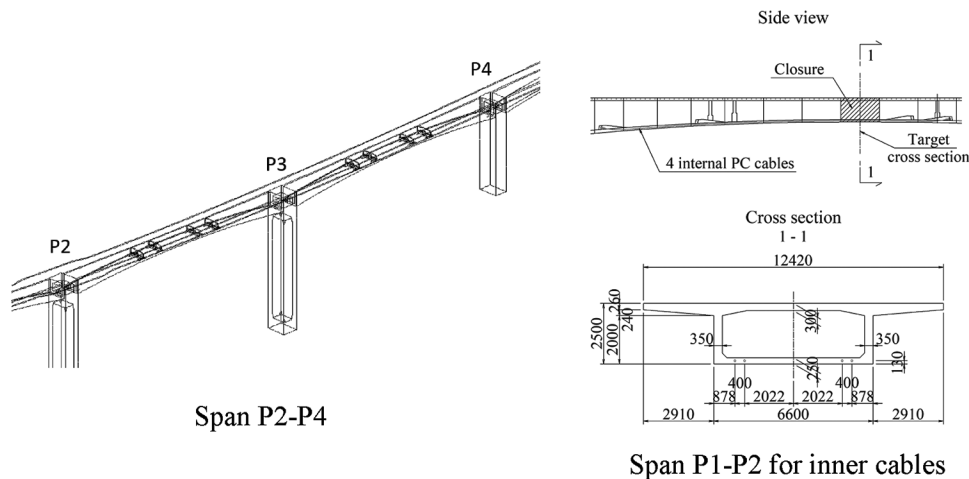


Fig. 11—PC steel profiles between span P2-P4 and span P1-P2 for internal cables.

extended over the whole span with a length of over 90 m, and this observation is quite contrary to the basic assumptions of the Japan Road Association⁸ or the DIANA manual, which assume a mirror inversion relief line of prestressing in the limited length of a span that is determined so that the integrated stress value becomes a stipulated seating value. In contrast to the assumption in DIANA, we assumed the steel force distribution as

$$f(s) = f^*(s/s_0^*) = \mu \left(\frac{1}{s_0^*} \right) \frac{\partial \theta}{\partial s} + \lambda \left(\frac{1}{s_0^*} \right) \quad (27)$$

and $T(s) = T_0 \cdot e^{-\mu \theta(s/s_0^*) + \lambda (s/s_0^*)}$ with $s_0^* = 3.3$ cm.

The results are shown in Fig. 13(b) and (c). Note that the tension force data represent the relieved portion of the total tension force surprisingly well, because it was considered that the observed total tension force in span P2-P4 has some irregularity. The results show good agreement with the observed tension force data, which suggests that stress relief for prestressing PC steels after seating may be possible with this steel stress distribution assumption.

As for the observation of the strain distribution in PC steels between P1 and P2, Fig. 14 shows a comparison of the PC steel force at prestressing and after seating between the observed and calculated values assuming friction coefficients of $\mu = 0.055$ and $\lambda = 0.0005$ and the same contact

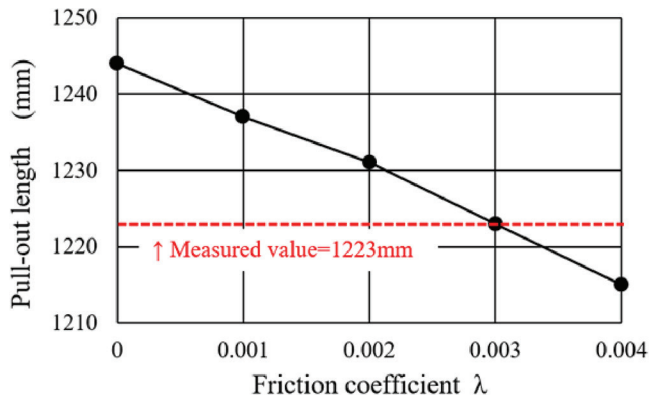


Fig. 12—Comparison of actual measured values and analysis values of pulled-out length of PC steel by prestressing.

Table 8—Analytical conditions for seating analyses

Property	Span P1-P2, internal cables	Span P2-P4
PC steel area, mm ²	1664.4	2635.3
Young's modulus, N/mm ²	191,900	194,150
Seating amount, mm	Side P1: 8.6 Side P2: 8.6	Side P2: 11.6 Side P4: 11.6
Tension at the ends, kN	2177	3472

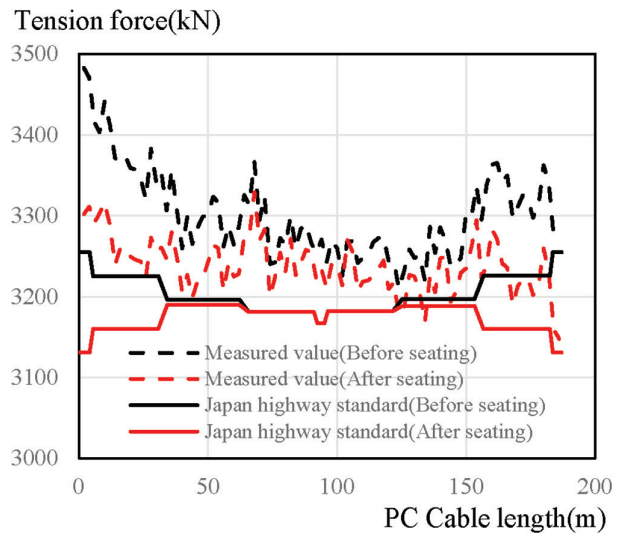
length index s_0^* of 3.3 cm. These results show almost perfect agreement between the observed and the calculated tension force values.

CONCLUSIONS

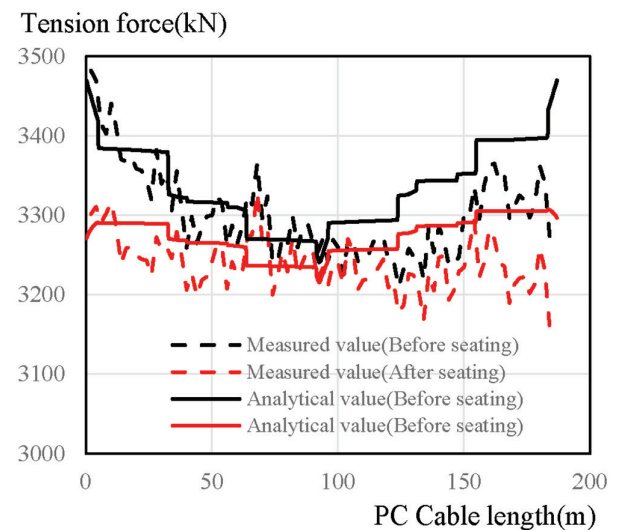
The reliability of the proposed three-dimensional (3-D) finite element method (FEM) analysis for prestressing was evaluated. One of the key issues to assure reliability is how to convert the prestressing force of PC steels with arbitrary configurations to frictional force and pseudo-centripetal force, and this was successfully achieved by polylinear approximation of the cable profile in 3-D space. The other issue is the assumption of the steel force distribution that considers friction and pseudo-centripetal force. It is very evident that smaller straight-line lengths in the polylinearization of the PC steel profile produce more accurate solutions. The accuracy of the results of the proposed method was also compared with the results of the two-dimensional (2-D) conventional method for a typical three-span continuous PC rigid-frame box-girder bridge. Further, the pulled-out length of PC steels and the PC steel strain that were observed in an existing six-span curved elevated bridge were compared with the calculated values, and the reliability of the method was confirmed. The present results are intended to improve the current analytical practice by using the 3-D FEM developed herein.

AUTHOR BIOS

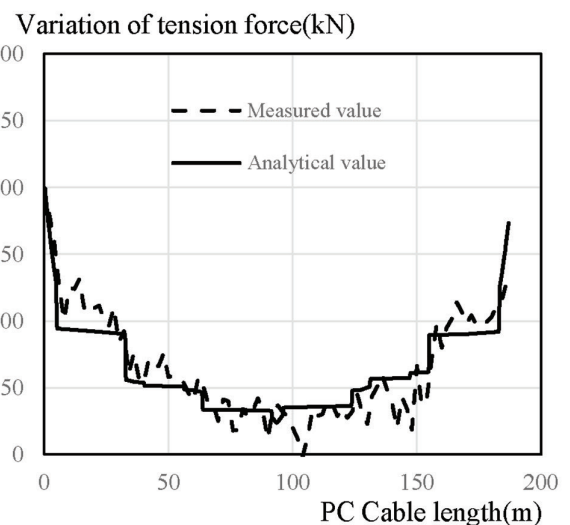
Yasuaki Ishikawa is a Professor at Meijo University, Nagoya, Japan. He received his engineering doctorate from Nagoya University, Nagoya, Japan. His research interests include constitutive laws for cracked concrete, and the mechanical behavior of prestressed concrete structures and its numerical simulation.



a) Total tension force(Japan Road Association)

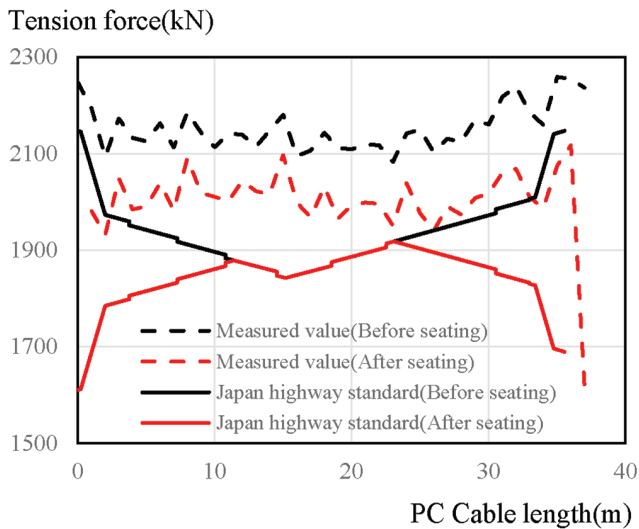


b) Total tension force(the proposed method)

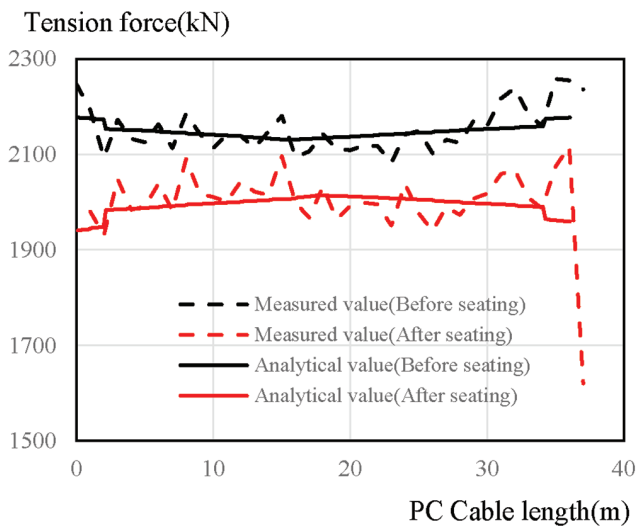


c) Variation of tension force before and after seating(the proposed method)

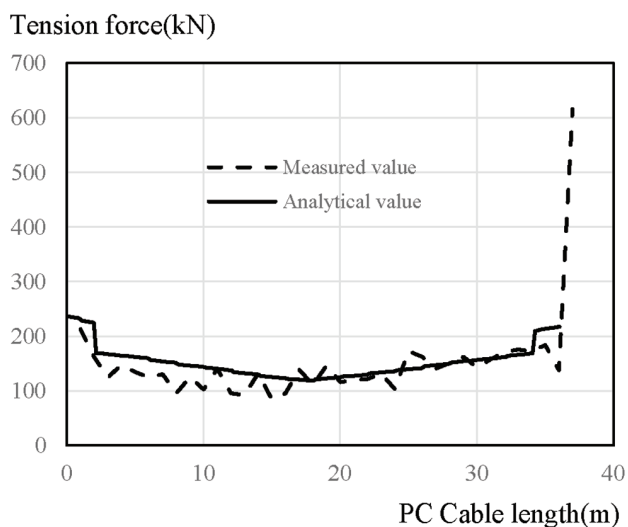
Fig. 13—Comparison of tension force distribution in span P2-P4.



a) Total tension force(Japan Road Association)



b) Total tension force(the proposed method)



c) Variation of tension force before and after seating(the proposed method)

Tomoki Ito is General Manager of the Vessel Engineering Department, Abe Nikko Kogyo Co., Ltd. He received his master's degree in engineering from Gifu University, Gifu, Japan.

Satoshi Hayakawa is Chief of the Design Section, Fuji P.S. Corporation. He received his Bachelor of Science degree from Meijo University.

ACKNOWLEDGMENTS

This study was conducted as part of the research activities of the LECOM Study Group. T. Tanabe, Professor Emeritus of Nagoya University, and the study group members provided many comments. T. Endo, Professor Emeritus of Tohoku Gakuin University; Y. Sasaki, former Director of Road Construction Division, Tohoku Regional Development Bureau, Ministry of Land, Infrastructure, Transport and Tourism; H. Osawa, Director; K. Temamoto, Assistant Director; and N. Sogabe, Technical Research Institute, Kajima Corporation, provided a wide variety of valuable data, including optical fiber measurement data and valuable comments on the actual bridge. Finally, the authors would like to express their deepest gratitude to Y. Imai of Fuji Consultants for providing them with many materials on overseas tension management. This study was supported by the Japan Society for the Promotion of Science under KAKENHI Grant Number JP23K03996.

REFERENCES

- Hamada, Y.; Inoue, M.; Kobayashi, A.; Takagi, N.; and Kojima, T., "Development of PC Truss Beams with Cylindrical Continuous Fiber Reinforcement Diagonal," *Doboku Gakkai Rombunshuu*, V. 2002, No. 697, 2002, pp. 25-37. doi: (in Japanese)10.2208/jscej.2002.697_25
- Takeda, K.; Tanaka, Y.; Shimomura, T.; Yamaguchi, T.; Kuga, S.; Ibayashi, K.; and Murakami, Y., "Loading Test and Numerical Evaluation of the Residual Strength of Pre-Tension PC Beam Affected by Chloride Attack," *Journal of the Japan Society of Civil Engineers, Ser. E2*, V. 71, No. 4, 2015, pp. 303-322.
- Ishikawa, Y., and Watanabe, K., "A Numerical Study on the Accuracy of Prestressing Analysis with Initial Strain Method," *The 79th JSCE Annual Meeting Proceedings*, Japan Society of Civil Engineers, Tokyo, Japan, 2024
- Okubo, K.; Imai, M.; Sogabe, N.; Nakae, S.; Chikiri, K.; and Niwa, J., "Development of the Measuring Method for PC-Tensile Force Distribution by Optical Fiber Applicable to Control of Prestressing and Maintenance of PC Structures," *Journal of the Japan Society of Civil Engineers, Ser. E2*, V. 76, No. 1, 2020, pp. 41-54. doi: 10.2208/jscejmcs.76.1_41
- Nagumo, H.; Mouri, K.; Morita, Y.; Sogabe, N.; Imai, M.; and Sato, T., "Construction of Tsukidate Viaduct Superstructure as Part of Reconstruction Assistance Road," *Bridge and Foundation Engineering*, V. 50, No. 12, 2016, pp. 5-10. (in Japanese)
- Ishikawa, Y.; Mizobuchi, T.; and Tanabe, T., "Development of FEM Thermal Analysis for Concrete Structures with Pipe Cooling System," *Mechanics and Physics of Creep, Shrinkage, and Durability of Concrete: A Tribute to Zdeněk P. Bažant*, 2013, pp. 491-498.
- Ishikawa, Y.; Nishio, H.; and Yagi, Y., "Development on New 3DFEM Analytical Method and Management in Prestressing Process for PC Structures," *Japanese Journal of JSCE*, V. 79, No. 10, 2023, pp. 1-16. (in Japanese) doi: 10.2208/jscej.23-00003
- Japan Road Association, "Specification for Highway Bridges, Part III: Concrete Bridges," Tokyo, Japan, 2017.
- Robitaille, S.; Bartlett, F. M.; and Youssef, M. A., "Evaluating Prestress Losses during Pretensioning," *Canadian Society for Civil Engineering Annual Conference*, St. Johns, NL, Canada, 2009.
- LECOM Research Association, <https://jnlecom.com/>. (in Japanese) (last accessed Jan. 13, 2025)
- Miyoshi, T., and Kato, H., "Structural Mechanics for Engineers: Bending Deformation and Shear Deformation (Part 1)," <https://www.akashi.ac.jp/miyoshi/>, 2015. (in Japanese) (last accessed Jan. 13, 2025)
- Nishio, H.; Yagi, Y.; and Ishikawa, Y., "Prestress Analysis of Large Three-Dimensional Systems and Prestress Management," *ACI Structural Journal*, V. 121, No. 5, Sept. 2024, pp. 109-122.

Fig. 14—Comparison of tension force distribution in span P1-P2 internal cables.